Combined pigment and metatranscriptomic analysis reveals synchronized diel patterns of phenotypic light response across domains in the open ocean

Kevin W. Becker^{1,§,*,*}, Matthew J. Harke^{2,§,‡}, Daniel R. Mende^{3,#}, Daniel Muratore^{4,5}, Joshua S. Weitz^{4,6}, Edward F. DeLong^{3,7,8}, Sonya T. Dyhrman^{2,9} and Benjamin A.S. Van Mooy¹

- ¹Department of Marine Chemistry and Geochemistry, Woods Hole Oceanographic Institution,
- 8 Woods Hole, MA, USA.
- ²Lamont-Doherty Earth Observatory, Biology and Paleo Environment, Columbia University,
- 10 Palisades, NY, USA.
- ³Daniel K. Inouye Center for Microbial Oceanography Research and Education (C-MORE),
- 12 University of Hawaii at Manoa, Honolulu, HI, USA.
- ⁴School of Biological Sciences, Georgia Institute of Technology, Atlanta, Georgia, USA.
- ⁵Interdisciplinary Graduate Program in Quantitative Biosciences, Georgia Institute of
- 15 Technology, Atlanta, Georgia, USA.
- ⁶School of Physics, Georgia Institute of Technology, Atlanta, Georgia, USA
- ⁷Department of Civil and Environmental Engineering, Massachusetts Institute of Technology,
- 18 Cambridge, MA, USA.
- 19 *Department of Biological Engineering, Massachusetts Institute of Technology, Cambridge, MA,
- 20 USA.

22

25

1

2

3

6

- ⁹Department of Earth and Environmental Sciences, Columbia University, New York, NY, USA.
- 23 §Equal contribution
- *Corresponding author: Kevin W. Becker, E-mail: kbecker@geomar.de
- [†]Present address: Division of Marine Biogeochemistry, GEOMAR Helmholtz Centre for Ocean
- 27 Research Kiel, Kiel, Germany
- 28 [‡]Present address: Gloucester Marine Genomics Institute, Gloucester, MA, USA
- 29 *Present address: Department of Medical Microbiology, Amsterdam University Medical Center,
- 30 Amsterdam, The Netherlands

Abstract

31

32

33

34

35

36

37

38

39

40

41

42

43

44

45

46

47

Sunlight is the most important environmental control on diel fluctuations in phytoplankton activity. and understanding diel microbial processes is essential to the study of oceanic biogeochemical cycles. Yet, little is known about the in situ frequency of phytoplankton metabolic activities and their coordination across different populations. We investigated the diel orchestration of phytoplankton activity involved in photosynthesis, photoacclimation, and photoprotection by analyzing the pigment and guinone distribution in combination with metatranscriptomes in the surface waters of the North Pacific Subtropical Gyre (NPSG). We found diel cycles in pigment abundances resulting from the balance of their synthesis and consumption. The night represents a metabolic recovery phase to refill cellular pigment stores, while the photosystems are remodeled towards photoprotection during the day. Transcript levels of genes involved in photosynthesis and pigment metabolism had highly synchronized diel expression patterns among all taxa, suggesting that there are similar regulatory mechanisms for light and energy metabolism across domains, and that other environmental factors drive niche differentiation. Observed decoupling of diel oscillations in transcripts and related pigments in the NPSG indicates that pigment abundance is modulated by environmental factors extending beyond gene expression/regulation, showing that metatranscriptomes may provide only limited insights on real-time photophysiological metabolism.

Introduction

48

49

50

51

52

53

54

55

56

57

58

59

60

61

62

63

64

65

66

67

68

69

70

71

Sunlight regulates the growth and cellular processes of all photosynthetic organisms in the ocean. It plays a pivotal role for ocean ecosystem processes, many of which are driven by energy provided by photosynthesis. The conversion of light into chemical energy is achieved by the absorption of photons by pigments in light-harvesting complexes followed by the transfer of that energy to the reaction center, where it is used to initiate the electron transfer and charge separation processes. Plastoquinones mediate the transfer of electrons between photosystem II (PSII), the cytochrome b_6 f complex (Cyt b_6 f), and photosystem I (PSI). The net result is the generation of ATP and NADPH, which are then used for carbon fixation, biosynthesis, and aerobic respiration (see review by Eberhard et al. [1]). Pigments play a central role in energy transport within light-harvesting complexes and photosystems of all photosynthetic organisms (Fig. 1). In particular, chlorophyll (Chl) is vital in these processes, performing both light harvesting and electron transfer, and it is typically the most abundant pigment. Carotenoid pigments also participate in energy transport and have an additional role in photoacclimation. Phytoplankton have developed a wide variety of pigment-based mechanisms for adapting to the variable light field experienced in the upper ocean. These mechanisms include downsizing of the photosynthetic antenna size by reducing the pool size of Chl, using xanthophyll cycling to arrest photoinhibition, and quenching singlet oxygen by carotenes [2]. Pigment molecules thus play key roles in the acclimation (short-term) and adaptation (long-term) of phytoplankton to the variability in light. In addition to their physiological importance, evolutionary divergence has led to the formation of a variety of chlorophyll and carotenoid pigments in different photosynthetic organisms, which allows us to delineate activity amongst phytoplankton groups [e.g., 3]. Also, the biosynthetic pathways of pigments are well known [e.g., 4]. This allows investigation of expression patterns of chlorophyll- and carotenoid pigment-related genes to gain further insight into the activity of individual phytoplankton groups, enabling taxonomic resolution not necessarily provided by pigment analysis alone.

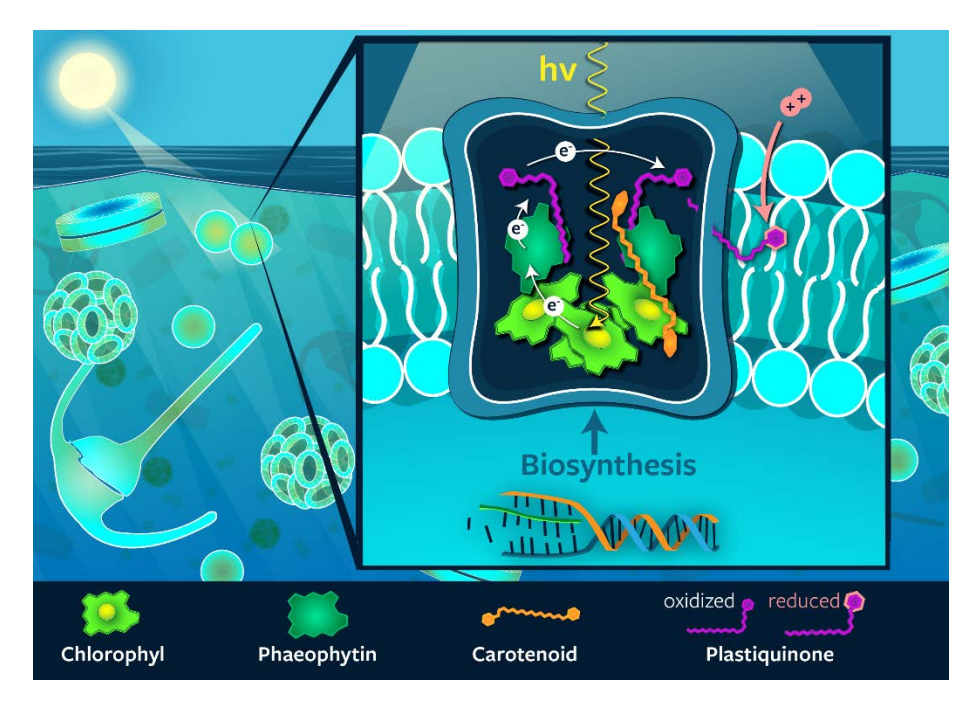


Fig. 1. Schematic representation of the structure of photosystem II in photosynthetic membranes. The relative locations of the major pigments and quinones as well as the pathway of electrons through these molecules is shown.

Diel oscillations in metabolic activities have been observed for both gene expression [e.g., 5–8] and pigment profiles [e.g., 9, 10] in natural phytoplankton populations. However, there has been no study of the relationship between phytoplankton pigments and photosynthesis-related gene expression over the diel cycle. Little is known about the synchronicity of photosynthetic metabolic pathways between different phytoplankton groups in nutrient deplete marine environments such as the subtropical gyres. Yet, the nutrient scarcity requires niche and/or resource partitioning by different phytoplankton to facilitate growth in the face of competition [11]. Additionally, temporal anomalies of phytoplankton biomass and cellular pigment content impact the optical properties of the surface ocean influencing the interpretation of satellite-derived ocean color observations and global models using these data [12]. In these studies, diel oscillations are typically not considered because satellite observations take place only at a narrow interval of the diurnal cycle. Instead, most global ocean ecosystem models based on satellite data assume that the observed

phytoplankton communities are under steady state growth conditions with respect to daily time-scales [e.g., 13]. Thus, better understanding group-specific differences as well as bulk community acclimation over the diel cycle is important for informing models relying on photoacclimation parameters to determine growth and accumulation rates as well as primary production [12, 14]. In this study, we used a combined analysis of pigments, quinones, and metatranscriptomes to investigate the diel orchestration of phytoplankton activity involved in photosynthesis, photoacclimation, and photoprotection in the surface waters of the North Pacific Subtropical Gyre (NPSG). An intensive multidisciplinary field campaign near station ALOHA in summer 2015 made use of a Lagrangian sampling strategy that mitigates the effect of spatial variability and allowed us to investigate microbial populations within the same water parcel over time [15]. In light of the importance of the subtropical gyres of the oceans for global biogeochemical cycles [16, 17], it is crucial to know how diel cycles of photoacclimation in phytoplankton affect the pigment composition in these ecosystems.

Results and discussion

Diel oscillations of chloropigments and carotenoids

The majority of detected pigment and quinone molecules investigated here displayed clear, statistically significant diel oscillations in abundance based on the Rhythmicity Analysis Incorporating Non-parametric Methods (RAIN) hypothesis-testing method ([15, 18, 19]; Supplementary Table 1). Diel oscillations of chloropigments, i.e., mono- and divinyl-Chls, showed maximum concentrations at dawn (6:00 h local time) and minimum concentrations during daylight hours (Fig. 2; Fig. S1). This pattern is distinct from previous investigations of diurnal Chl, which showed a mid-day maximum and a night-time minimum especially in data integrated through the water column [10, 20, 21]. Based on these previous observations, it was thought that Chl synthesis directly reflects primary production by photoadaptation, with increasing cellular chlorophyll during the day and chlorophyll break down (or dilution by cell division) at night [e.g., 22]. Alternatively,

116

117

118

119

120

121

122

123

124

125

126

127

128

129

130

131

132

133

134

135

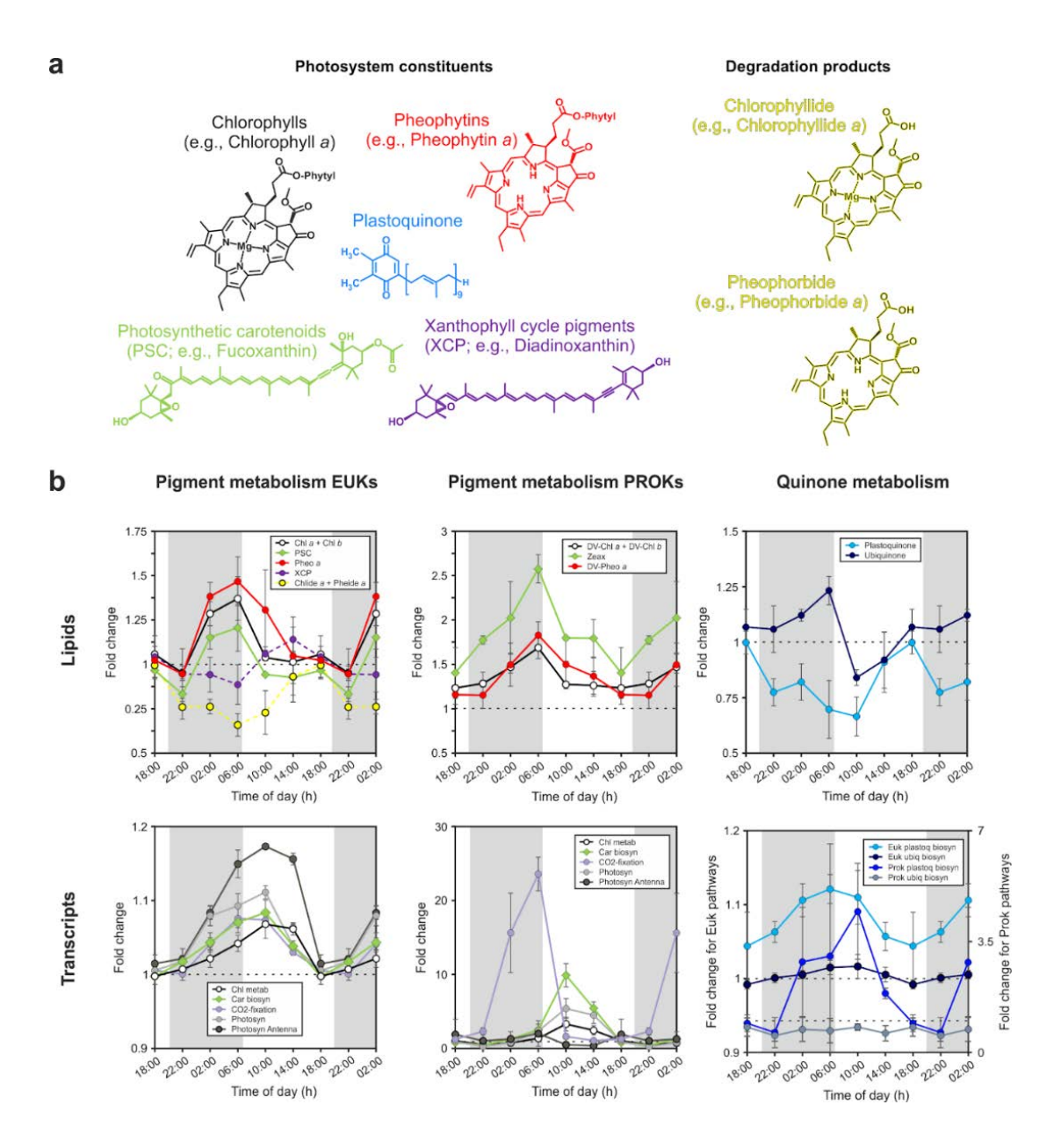
136

137

138

139

mid-day minima in surface water ChI that have frequently been observed in data from in vivo ChI fluorescence have been interpreted to result from non-photochemical quenching, not absolute decreases in Chl concentrations. The reasoning behind this interpretation is that variability in quantum yield for fluorescence is significant and complicates the interpretation of Chl estimates from in vivo fluorescence at high light intensities (e.g., [23-25]). However, here we used mass spectrometry to determine ChI concentrations from lipid extracts, which is insensitive to quenching. Other studies, measuring extracted ChI, also showed clear and reproducible nighttime maxima for both near surface waters (e.g., [9]) and culture experiments at high light intensities (e.g., [26-29]). Additionally, Fouilland et al. [30] found a depth-dependence of diel variations in Rubisco activity and Chl concentration per cell further supporting a light regime-dependence of Chl profiles. The photosynthetic carotenoids (PSC) aligned with ChI over the diel cycle (Fig. 2; Fig S1) and no periodic variations were observed in ratios among PSC pigments (Fig. S2), which has previously been observed for both phytoplankton cultures [31] and surface ocean samples [32] and is consistent with PSC and Chl having similar functions [33]. The most abundant PSC in surface waters were fucoxanthin (diatom biomarker), 19'-butanoyloxyfucoxanthin (pelagophyte biomarker), and 19'-hexanoyloxyfucoxanthin (prymnesiophyte biomarker). All showed similar trends, with a nocturnal increase leading to a pre-dawn maximum and a minimum later, during daylight hours (Fig. 2 and Fig. S2). Similar to Chls, the nocturnal increase may seem counterintuitive as light harvesting molecules are needed during the day for photosynthesis. However, at high photon flux, the rate of photon absorption by ChI antenna far exceeds the rate at which photons can be utilized for photosynthesis; to avoid over-excitation of the photosystem, high light acclimation typically involves downsizing of the antenna of both photosystems [34, 35], in particular of PSII [36]. The observed profiles thus likely represent the balance of photoprotective and photorepair mechanisms.



investigated pigments and respiratory quinones associated with the photosystem. **b** Time-of-day average of fold change relative to 18:00 h (local time) of chloro- and carotenoid pigments, quinones, as well as transcript associated with the metabolism of the pigment and quinone molecules. Error bars represent the standard deviation of averaged values for each time of day (n≥6). Molecular structures and pigment and quinone data are colored according to compound group. If colors for transcripts match those of pigments or quinones, transcripts are related to the metabolism of the respective molecule.

While the observed depression in Chl and PSC during daylight might be explained by PSII damage due to high-light stress, the increase at night clearly indicates synthesis in the dark. Increased vertical mixing during the night could also explain this signal, but the surface mixed

Fig. 2. Diel oscillations of pigments and pigment-related transcripts. a Molecular structure of

153

154

155

156

157

158

159

160

161

162

163

164

165

166

167

168

169

170

171

172

173

174

175

176

layer typically ranges from ~0-40 m [37], which is too shallow to transport large amounts of Chl, for example, from the deep ChI maximum (at ~100 m at station ALOHA our sampling site and times [15, see Fig. 1 therein]) to the sampling depth of 15 m. Additionally, *Prochlorococcus* cell numbers remained constant over the diel cycle in our samples, which results in increasing divinyl-Chl/cell guotas during the night (Fig. S2) and supports the hypothesis of night-time synthesis. The energy and carbon for the *de novo* synthesis of Chls in the dark is likely provided by carbon stores, for example glycogen in cyanobacteria or triacylglycerols (TAGs) in eukaryotic phytoplankton. Consistent with this, we recently showed that nanoeukaryotic phytoplankton in the NPSG accumulate large amounts of TAGs during the day and subsequently consume them at night [38]. A similar mechanism has been proposed for dark synthesis of proteins in several phytoplankton (e.g., [39-41]) and our findings extend the potential utilization of C stores by phytoplankton for dark synthesis of pigments. Pheophytin and divinyl- pheophytin profiles were tightly coupled to those of ChI and divinyl-ChI, respectively, with peak times at night (Fig. 2). While the presence of pheophytin in marine samples has traditionally been interpreted to reflect dead or dying cells due to the high abundance of these pigments in zooplankton guts and sinking particles, which are unlikely to be consistently captured in our small volume samples [42-46], we hypothesize that the pheophytins may in fact be associated with living phytoplankton. Most notably, pheophytin has been found to play an important role in electron transport in PSII by being the primary electron acceptor for excited ChI [47] and has been frequently detected in isolated PSII with a 6:2 stoichiometry of Chl and pheophytin [e.g., 48]. Additionally, pheophytin and Chl share a biochemical pathway, where Chl is converted to pheophytin by a magnesium dechelatase [49] supporting the idea of simultaneous dark synthesis of Chls and pheophytins. Other Chl related structures, pheophorbide and chlorophyllide, were out of phase with Chl and pheophytin, both showing peak times at 14:00 h (Fig. 2). These Chl related structures are not known to participate in photosynthetic reactions, suggesting daytime peaks are likely associated with photodamage and photoprotective

177

178

179

180

181

182

183

184

185

186

187

188

189

190

191

192

193

194

195

196

197

198

199

200

201

202

mechanisms. High light stress during daylight is also apparent from xanthophyll cycle pigments, essential molecules that channel excess energy away from chlorophylls for protection against photooxidative damage [50]. Diadinoxanthin (Dd) and diatoxanthin (Dt), which are part of the Dd/Dt xanthophyll cycle predominantly possessed by haptophytes, diatoms and dinoflagellates in the NPSG [51], were the most abundant xanthophyll cycle pigments detected (Fig. S1). The sum of Dt and Dd showed clear diel cycles with maximum abundances during the day (peak time at 14:00 h; Fig. 2). This pattern indicates that the cellular xanthophyll pigment pool increased during daylight hours likely due to photoadaptation triggered by a change of light intensity over the course of the day [32]. The de-epoxidation state (DES), which is defined as [Dt]/[Dt+Dd], showed a minimum during the day (Fig. S2), which contrasts observations from culture experiments [52] and the field [32]. This pattern is likely related to severe high-light stress at 15 m water depth where our samples were collected. Oxidative stress due to an increased formation of various ROS species consumes Dt by degrading it to low molecular weight compounds [53, 54], requiring resynthesis for the pool to be refilled. Potentially, phytoplankton refill cellular Dt stores during the night. We therefore looked for Violaxanthin de-epoxidases, which convert Dd to Dt in the xanthophyll cycle [55], and find that transcript abundances for the diatoms and haptophytes were out of phase with XCPs (Fig. S10). Additionally, Zeaxanthin epoxidases, which participate in nonphotochemical guenching by regulating the level of epoxy-free xanthophylls in photosynthetic energy conversion, showed statistically significant diel oscillation for diatoms and haptophytes with peak times during the day at 10:00 h local time (Fig. S11). Our results from the pigment analysis thus show that high light conditions in the upper photic zone results in severe photooxidative stress for phytoplankton, which is displayed in a distinct and different diel xanthophyll cycle pigment and ChI degradation product patterns compared to observations from the deeper photic zone [32]. Through this, phytoplankton are likely able to maintain the balance between dissipation and utilization of light energy to minimize the generation of ROS and resulting molecular damage. Since net primary production is typically invariable throughout the mixed layer at station ALOHA [56], the observed pigment signal represents a light adaptation signal as opposed to an increased photodegradation state of near surface phytoplankton cells.

Diel patterns of isoprenoid quinones

203

204

205

206

207

208

209

210

211

212

213

214

215

216

217

218

219

220

221

222

223

224

225

226

227

Analyses of quinones in the marine water column are still relatively rare [38, 57, 58], but due to their physiological importance in electron transport in both photosynthesis and cellular respiration, quinones provide valuable information on microbial activities. While plastoquinones (PQs) are primarily involved in electron transport of PSII, ubiquinones (UQs) are associated with aerobic respiration [59]. Recent studies suggested PQs and UQs might additionally be involved in photoprotective mechanisms by acting as ROS scavengers [60-63]. In our samples, both quinone groups showed distinct and statistically significant diel patterns (Fig. 2; Table S1) with UQs peaking at the end of the night (6:00 h; cf. [38]) and PQs peaking at the end of the day (18:00 h, Fig. 2). These two groups of structurally similar molecules were thus out of phase by 12 h. The pre-dawn maximum of UQs is likely associated with enhanced respiration of storage lipids, which have been shown to accumulate during the day and are consumed at night [38]. The daytime increase of PQs may partly be driven by growth, but similar to other photosystem constituents, photoacclimation mechanisms play a major role for intercellular PQ abundances. Increasing the rates of electron transport processes can protect PSII when absorption of quanta exceeds the requirements of photosynthetic carbon metabolism [64], which, in turn, requires an increase in the PQ pool size and may in part be responsible for observed daytime maxima of PQs. Additionally, in plants, PQs have been shown to act as ROS scavengers under high-light stress [65, 66]. These processes deplete PQs due to photooxidation during daylight hours. Hence, they have to be resynthesized to keep this important function. The daytime increase in the proportion of the PQ to chlorophyll pool (Fig. S2) is likely due to the different organization of chloroplast structure. In plants, chloroplasts have less antenna chlorophyll per electron transport chain under high light than low light [67].

Diel oscillations of transcripts involved in photosynthesis

228

229

230

231

232

233

234

235

236

237

238

239

240

241

242

243

244

245

246

247

248

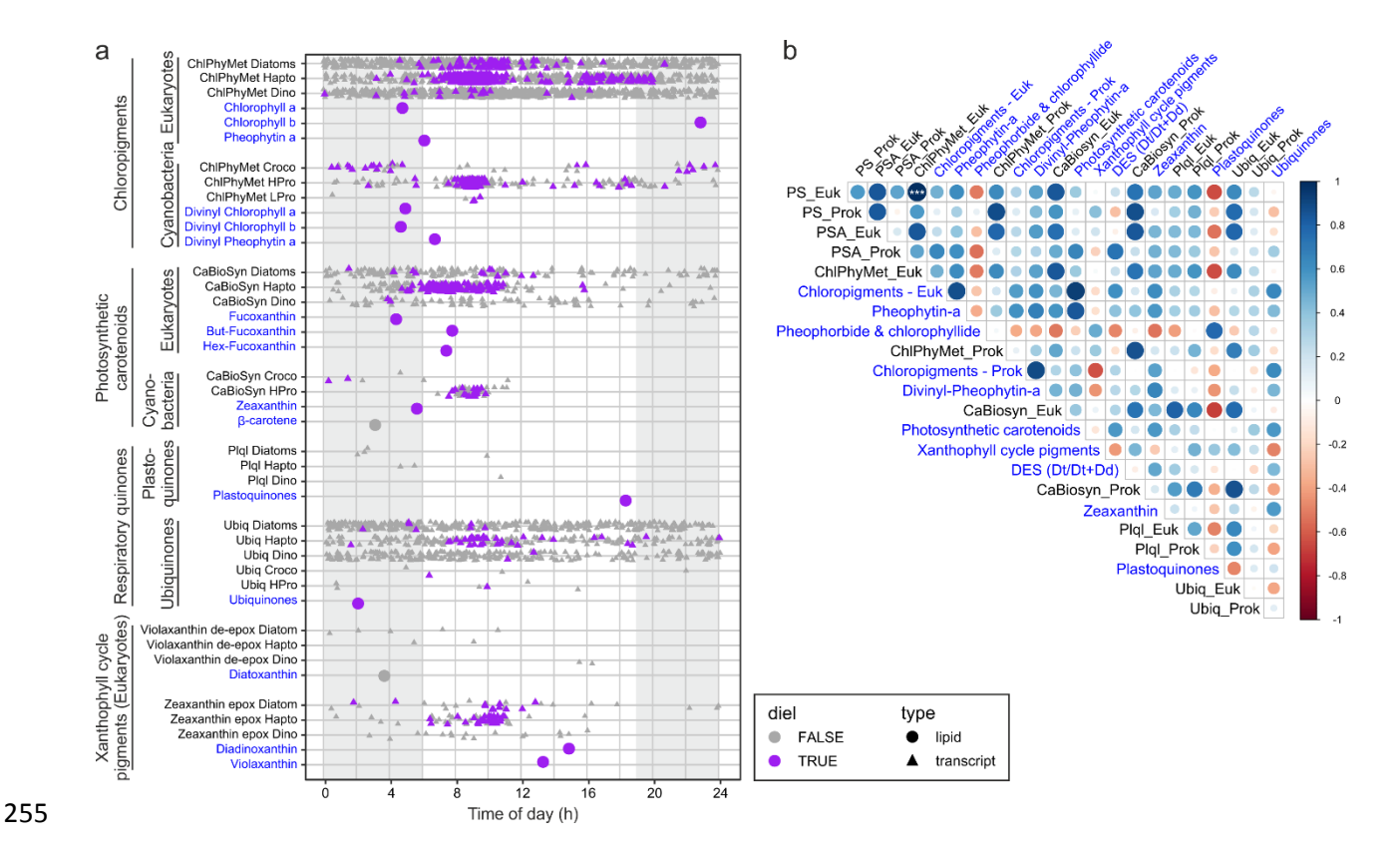
249

250

251

252

In addition to measuring diel oscillations in pigments and quinones, we further explored diel transcriptional rhythms of genes involved in photosynthesis and pigment metabolism of the dominant bacterial and eukaryotic groups at station ALOHA. Transcripts of all photosynthetic populations showed statistically significant diel oscillations for most investigated pathways (Supplementary Table 2). Almost all significant diel transcripts associated with photosynthesis and pigment metabolism peaked in the first part of the day (10:00 h; Fig. 3a), suggesting their transcriptional regulation in phototrophs is strongly synchronized across diverse taxa (within the temporal resolution of our measurements). These observations further imply that the pigment metabolism network is conserved across domains in the oligotrophic open ocean (see Figs. S3 – S9 for profiles of individual phytoplankton groups). This complements recent findings by Kolody et al. in coastal systems [8] who observed periodic photosynthesis-related transcripts that were conserved across diverse phototrophic lineages in a high-nutrient coastal environment. Thus, our data is consistent with a multispecies synchronous diel cycles of genes associated with photosynthesis and pigment metabolism with increasing transcript abundances during dark hours and peak times in the mid-morning. Nightly expression of photosynthesis genes in natural photoheterotrophic bacteria, followed by a drawdown shortly after light onset, has been suggested to be related to preparing cells for efficient solar energy harvest in the early morning hours [6]. Our data from cyanobacteria and eukaryotic phytoplankton and consistent with this hypothesis. A notable exception of this pattern was Crocosphaera. Transcripts for most pathways in this diazotroph only showed a weak relationship or no significant positive correlation with the pathways in the other phytoplankton populations. However, this is in agreement with other culture [68] and field-based observations [15, 69]. The process of N₂ fixation in this unicellular cyanobacteria seems to require a tightly orchestrated diel cycle distinct from other diazotrophs and nondiazotrophic microorganisms [15, 69].



transcripts and actual pigment abundances **a**. Peak times of expression of all transcripts assigned to KEGG pathways associated with pigment metabolism (triangles) and pigment molecule abundances (circles). Purple symbols denote transcripts or pigment molecules identified as significantly periodic (24-hour period) whereas gray symbols denote peak times without a significant diel component in peak expression or pigment abundance, respectively. **b**. Spearman's rank correlation matrix of the different pigment and quinone classes (blue text) and aggregated genes within the KEGG pathways Photosynthesis (PS), Carotenoid biosynthesis (CaBiosyn), Chlorophyll and porphyrin metabolism (ChlPhyMet), Photosynthesis - antenna proteins (PSA), Plastoquinol biosynthesis (PIql), Ubiquinone and other terpenoid-quinone biosynthesis (Ubiq) separated into prokaryotes (Prok) and eukaryotes (Euk).

Strong diel rhythmicity in transcripts of eukaryotic phytoplankton including haptophytes and diatoms is expected from earlier culture and field experiments [e.g., 5, 8, 19, 70–72]. However, peak times for pathways involved in photosynthesis and pigment metabolism seem to be variable in culture experiments. For example, light harvesting antenna protein gene expression was enriched in late afternoon (2 to 6 pm) for iron-replete cultures of the diatom *Phaeodactylum*

Fig. 3. Relationship between periodic pigment-associated gene expression in phytoplankton

tricornutum, along with genes involved in porphyrin and chlorophyll metabolism [71], while enrichment for the KEGG pathways photosynthesis and porphyrin and chlorophyll metabolism was observed in the dawn for the diatom *Thalassiosira pseudonana* [70]. This variability in the timing of gene expression contrasts our findings from natural phytoplankton populations in the NPSG, which showed synchronized expression patterns across diverse phytoplankton. This synchrony across taxa has recently also been shown for a coastal environment [8] and together the results indicate that responses to signals in the environment, possibly including organismal interactions, play an important role in shaping gene expression patterns of natural phytoplankton populations.

Decoupling between transcription and pigment production

The combination of pigment analysis and metatranscriptomics further shed light on the complex interplay between metabolic pathways and actual metabolite concentrations. In a previous study of energy storage mechanisms of natural phytoplankton populations at station ALOHA, we showed that gene expression and lipid abundances were decoupled - despite distinct diel patterns in storage lipid abundance, transcript abundance for the genes involved in the final step of their biosynthesis remained relatively constant over the diel cycle [38; Fig 4]. In addition, the correlations we observe between transcripts and lipids (shown in Fig. 3b) are not significantly stronger than the correlations expected from comparing independent time series (see Fig. S13). In culture experiments with the marine diatom *Phaeodactylum tricornutum*, during high light acclimation, ChI metabolism at the transcriptional level was down-regulated at an early stage while ChI a concentrations showed a lag time to this initial transcriptional response [73], which is what would be expected for an ideal system. However, the change of concentrations of pigments or any metabolite is governed by the difference between production and consumption. For example, the observed offset in peak time between transcripts (mid-morning) and associated pigments (dawn, Fig. 3a) suggests the influence of additional regulatory processes for chlorophyll and carotenoid

298

299

300

301

302

303

304

305

306

307

308

309

310

311

312

313

314

315

316

317

318

319

320

321

322

pigment abundances. Irradiance at 15 m at station ALOHA (700 µmol m⁻² s⁻¹) was higher than in the "high light" experiments conducted by Nymark et al. [73] (500 µmol m⁻² s⁻¹) and the different patterns between the culture experiments and our field based observations may be related to photoacclimation mechanisms. Our observations that transcripts peak approximately 4 hours later than their corresponding pigments might indicate that phytoplankton actively synthesize Chls and PSC at a high rate, but catabolic processes, i.e., a shift towards photoprotection, consume more molecules than are produced. Our data thus show that metatranscriptome data should not be interpreted as a real-time readout of photophysiological metabolism. The response of cells towards ambient light conditions involves optimization of their photosystems in such a way that energy generation and utilization are in balance. Kana et al. [74] proposed that pigment abundance is modulated by environmental factors extending beyond gene expression/regulation, i.e., the initial response to high light intensities is self-adjusting. The light sensor that in a first step regulates photoacclimation in phytoplankton has been suggested to be the redox state of the guinone pool [74]. Although our methods do not allow direct determination of the redox state of the PQ pool because plastoquinols become spontaneously oxidized to plastoquinones when exposed to oxygen during sample analysis, we found significant diel oscillations in the expression of Chl a/b binding protein (cab) genes (Fig. S12). The cab genes are important for both light-harvesting and photoprotection in eukaryotic phytoplankton and are under transcriptional control by the redox poise of the PQ pool [75]. In cultures, under high light, it has been shown that the PQ pool becomes more reduced resulting in a suppression of cab mRNA synthesis and light harvesting complex production, and an ultimate decrease in cellular photosynthetic pigments [75]. We observed a decline in cab transcript abundances during daylight hours (Fig. S12) suggesting that this light intensity-dependent photon-sensing system is active in the NPSG. This process then likely triggers the down-regulation of photosynthesis and pigment metabolism related genes to keep pigments levels consistently low to prevent over-excitation of the photosystems at the high irradiance levels phytoplankton experience in the surface waters of the NPSG. Besides the insights our data provided on the (de)coupling between transcriptional and metabolite rhythms, our data suggest that the night reflects a metabolic recovery phase that is used by all photosynthetic organisms across domains to be prepared for photosynthetic reaction as soon as the sun rises, make optimal use of sunlight energy and grow efficiently.

Conclusions

323

324

325

326

327

328

329

330

331

332

333

334

335

336

337

338

339

340

341

342

343

344

345

346

347

We are just beginning to understand in detail the mechanisms by which marine phytoplankton are able to maintain homeostasis and coordinate growth under metabolic and energetic shifts driven by the perpetual rising and setting sun. Our work demonstrates that combined lipidomics (here pigment and quinone profiles) and transcriptomics can provide mechanistic insights into rapid (i.e., sub-daily) microbial processes (Fig. 4). While pigments involved in light harvesting and energy transfer peaked at dawn, photoprotective pigments and ChI degradation products peaked later in the day. This succession of pigment metabolism according to their function suggests a recovery of cellular ChI and PSC stores at night and a dominance of photoprotective mechanisms during daylight. The diel cycles of combined pigment, guinone and transcriptomics data from the NPSG thus highlight the fundamental connection between sunlight and phytoplankton photosynthetic metabolism [74]. Furthermore, diel metabolic cycles were similar across all major phytoplankton taxa with few exceptions. Thus, harvesting light energy is not the basis for temporal niche differentiation among these taxa, which stands to reason because photons are in excess at 15 m depth and therefore are not a resource that phytoplankton compete with one another to obtain. Niche differentiation among phytoplankton occurs for processes involving competitive and growthlimiting substrates, such as nutrients, which are scarce in the surface of the oligotrophic ocean. Yet the daily synthesis of pigments - and the machinery required for this synthesis - place considerable burden on phytoplankton for growth-limiting substrates. Thus, any temporal partitioning in accessing growth-limiting substrates must also be accompanied by different modes for their storage, which are rarely considered [77, 78]. In summary, the data presented herein advances our knowledge of this fundamental process within photosynthetic microbes in the mixed layer, providing valuable detailed observations of transcriptional and pigment dynamics across kingdoms. These data will thus prove useful for future models linking remotely sensed ocean color to temporal dynamics of pigment concentrations or photosynthetic activity.

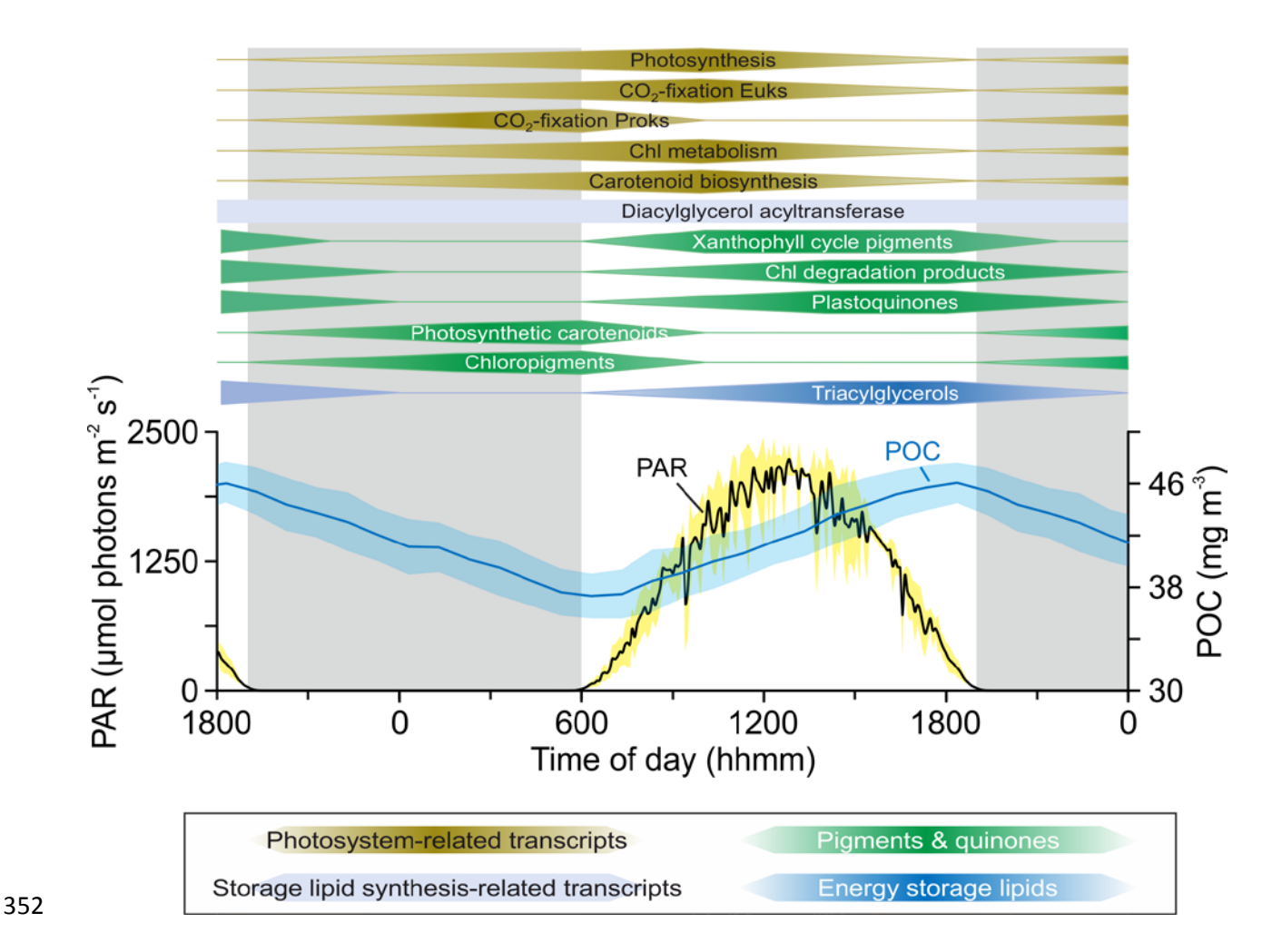


Fig. 4. Conceptualized temporal separation of phytoplankton pigment, plastoquinone and transcript abundances during the dark-light cycle in surface waters (15 m) at station ALOHA. The timing was set based on Fig. 2 with the center of the polygon indicating the approximate peak time. Additionally, the particulate organic carbon (POC) and Photosynthetically Available Radiation (PAR) profiles averaged for one day/night cycle are shown. Surface PAR data was obtained from the HOT program database (http://hahana.soest.hawaii.edu/hoelegacy/hoelegacy.html), POC data from White et al. [76] and TAG (Triacylglycerols & Diacylglycerol acyltransferase) data from Becker et al. [38].

Materials and methods

362

363

364

365

366

367

368

369

370

371

372

373

374

375

376

377

378

379

380

381

382

383

384

385

386

Sample collection and lipid analysis. Seawater samples were collected during R/V Kilo Moana cruise KM1513 (July/August 2015) near Station ALOHA (22°45'N, 158°00'W) in the oligotrophic North Pacific Subtropical Gyre using standard Niskin-type bottles attached to a CTD rosette. Samples were collected every 4 h from 2 p.m. (local time) July 27, 2015 to 6 a.m. (local time) on July 30, 2015. Samples (~2 L) were filtered using vacuum filtration (ca. -200 mm Hg) onto 47 mm diameter 0.2 µm hydrophilic Durapore filters (Millipore). Samples were immediately flash-frozen and stored at -196 °C until processing. Lipids were extracted using a modified Bligh and Dyer protocol [79] with DNP-PE-C_{16:0}/C_{16:0}-DAG (2,4-dinitrophenyl phosphatidylethanolamine diacylglycerol; Avanti Polar Lipids, Inc., Alabaster, AL) used as an internal standard. Filter blanks were extracted and analyzed alongside environmental samples. The total lipid extract was analyzed by reverse phase high performance liquid chromatography (HPLC) mass spectrometry (MS) on an Agilent 1200 HPLC coupled to a Thermo Fisher Exactive Plus Orbitrap high resolution mass spectrometer (ThermoFisher Scientific, Waltham, MA, USA). HPLC and MS conditions are described in detail in [38] and [80]; modified after [81]. For identification and quantification of pigments and quinones, we used LOBSTAHS, an opensource lipidomics software pipeline based on adduct ion abundances and several other orthogonal criteria [80]. Pigments and quinones identified using LOBSTAHS were quantified from MS data after pre-processing with XCMS [82] and CAMERA [83]. XCMS peak detection was validated by manual identification using retention time as well as accurate molecular mass and isotope pattern matching of proposed sum formulas in full-scan mode and tandem MS (MS2) fragment spectra of representative compounds [38]. For validation of accuracy and reliability of LOBSTAHS identification and quantification, quality control (QC) samples of known composition and spiked lipid standards were interspersed with samples as described previously [80]. Lipid abundances obtained from LOBSTAHS were corrected for relative response of commercially available standards. Abundances of quinones were corrected for the response of a ubiquinone (UQ_{10:10}) standard, chlorophylls and their associated compounds using a chlorophyll a standard, and carotenoid pigments using a β -carotene standard. All standards were purchased from Sigma Aldrich (St. Louis, MO, USA). Individual response factors were obtained from external standard curves by triplicate injection of a series of standard mixtures in amounts ranging from 0.15 to 40 pmol on column per standard. Data were corrected for differences in extraction efficiency using the recovery of the DNP-PE internal standard (Avanti Polar Lipids, Inc., Alabaster, AL; USA).

Eukaryotic metatranscriptome analysis.

387

388

389

390

391

392

393

394

395

396

397

398

399

400

401

402

403

404

405

406

407

408

409

410

411

Samples for the >5 µm microeukaryote metatranscriptomes were collected at the same time as lipid samples following Harke et al. [72]. Briefly, 20 L of seawater was collected in acid-washed carboys every 4 h from 10 p.m. (local time) July 26, 2015 to 6 a.m. (local time) on July 30, 2015 for a total of 21 time points. Seawater was prescreened through a 200 µm nylon mesh and then filtered onto two 5 μm polycarbonate filters (47 mm) via peristaltic pump, passing ~10 L across each filter. Samples were then flash frozen in liquid N until extraction. Total RNA was extracted from individual filter sets (n = 2 per timepoint) using Qiagen RNeasy Mini Kit (Qiagen, Hilden, Germany) as in Harke et al. [72] and then sequenced on an Illumina HiSeq 2000 at the JP Sulzberger Genome Center (CUGC) using center protocols. PolyA-selected samples were sequenced to a depth of 90 million 100 bp, paired-end reads. Raw sequence quality was visualized with FastQC (https://www.bioinformatics.babraham.ac.uk/projects/fastqc/) and cleaned and trimmed using Trimmomatic [84] version 0.27 (paired-end mode, 4 bp-wide sliding window for quality below 15, minimum length of 25 bp). Processed reads were mapped to a reference database after Alexander et al. [85], constructed from the Marine Microbial Eukaryotic Transcriptome Sequencing Project (MMETSP; [86]. Transcripts within the reference database were annotated with KEGG using UProC [87]. Mapping was conducted with the Burrows-Wheeler Aligner (BWA-MEM, parameters –k 10 –aM; [88]) and read counts generated with the HTSeq 0.6.1 package (options –a 0, --m intersection-strict, -s no; [89]). Read counts were filtered for contigs with average read counts ≥ 10 across the time series and then normalized with DESeq2 "varianceStabilizingTransformation" command [90]. These environmental sequence data are deposited in the Sequence Read Archive through the National Center for Biotechnology Information under accession no. SRP136571, BioProject no. PRJNA437978. To facilitate comparisons with pigment and quinone data, transcripts occurring in dinoflagellate, haptophyte, and diatom taxa were mined for the following KEGG pathways: Carotenoid biosynthesis [PATH:ko00906], Porphyrin and chlorophyll metabolism [PATH:ko00860], Photosynthesis [PATH:ko00195], Carbon fixation in photosynthetic organisms [PATH:ko00710], and Ubiquinone and other terpenoid-quinone biosynthesis [PATH:ko00130]. In addition, signals involved in plastoquinol biosynthesis were separated out from Ubiquinone and other terpenoid-quinone biosynthesis to mirror pigment and quinone data.

Prokaryotic metatranscriptome analysis

For this study, a previously published dataset of transcriptomes was used [15, 19], which consisted of bacterioplankton samples collected every four hours over the same study period. Sampling was performed as follows: 2 L of seawater were filtered onto 25 mm, 0.2 µm Supor PES Membrane Disc filters (Pall) using a peristaltic pump. The filtration time was between 15 and 20 min and filters were placed in RNALater (Ambion) immediately afterwards, and preserved at -80 °C until processing. Molecular standard mixtures for quantitative transcriptomics were prepared as previously described [91], and, 50 µl of each standard group was added to sample lysate before RNA purification. Metatranscriptomic libraries were prepared for sequencing with the addition of 5–50 ng of RNA to the ScriptSeq cDNA V2 library preparation kit (Epicentre). Metatranscriptomic samples were sequenced with an Illumina NextSeq 500 system using V2 high output 300 cycle reagent kit with PHIX control added. Reads were mapped to the station ALOHA gfne catalog [92]

using LAST [93]. Transcripts were quantified through normalization of raw hit counts using molecular standards [15]. Transcripts in *Prochlorococcus* and *Crocosphaera* were mined for the same KEGG pathways as the eukaryotes.

Statistical analysis

437

438

439

440

441

442

443

444

445

446

447

448

449

450

451

452

453

454

455

456

457

458

459

460

461

The statistical significance of diel oscillations of pigment, quinone and transcript abundances was tested using the RAIN package in R [see 15, 18, 19]. Resulting p-values from RAIN analysis were corrected for false discovery using the 'padjust' function in R with Benjamini-Hochberg method [94]. Corrected p-values ≤ 0.05 were considered to have significant diel periodicity. Peak times were calculated with a harmonic regression, fitting the expression data to a sine curve.

To evaluate rank correlations between pigment and transcript time series, data were centered to a mean of zero and scaled to one standard deviation to facilitate inter-comparability between data with different units. Then, pairwise spearman rank correlations (spearman's rho) were calculated between all pairs of measured time series. To address autocorrelation, we evaluated whether observed correlations were stronger than independent identically distributed random walks, which are known to often be spuriously correlated [95]. To test this, the differences between consecutive observations were calculated for all measured time series. The frequency distributions of observed differences were then used to bootstrap sample 20 random differences and cumulatively summed to simulate a random walk. This process was repeated and we bootstrap sampled 100,000 such random walks independently to create a null ensemble of time series with similar autocorrelation-1 structure to the data. Bootstrap sampling was then used to randomly select 100,000 pairs of random walks and rank correlations were calculated to generate a Monte Carlo simulation of the distribution of spearman's rho between independent identically distributed random walks with step sizes similar to those observed in the data (Fig. S13). This distribution was then used to calculate empirical one-tailed p-values of observed rank correlations. The adaptive Benjamini-Hochberg method was applied to account for multiple testing [94]. All calculations were carried out using the

463

464

465

466

467

468

469

470

471

472

473

474

475

476

477

R statistical computing language v 3.6.3 with functionalities from the 'tidyverse' set of packages version 1.2.1. Acknowledgement We are grateful to the officers and crew of the R/V Kilo Moana cruise KM1513 (HOE Legacy II). We thank Helen F. Fredricks for help with lipidomics analysis, and Daniel J. Repeta for help with onboard sample collection. This work was funded by a grant from the Simons Foundation (SCOPE, Award # 329108, B.A.S.V.M. S.T.D, E.F.D.), and Gordon and Betty Moore Foundation (grant #3777, E.F.D.). K.W.B. was further supported by the Postdoctoral Scholarship Program at Woods Hole Oceanographic Institution & U.S. Geological Survey. **Author contributions** B.A.S.V.M., S.T.D., E.F.D. conceived the study. K.W.B., M.J.H., and D.R.M. conducted and analyzed lipidomic, eukaryotic metatranscriptomic and prokaryote transcriptomic studies, respectively. J.S.W. and D.M. supported data analysis. K.W.B. and M.J.H. wrote the paper with contributions from all authors. **Competing interests** The authors declare no competing financial interests.

References

478

- 479 1. Eberhard S, Finazzi G, Wollman F-A. The Dynamics of Photosynthesis. *Annu Rev Genet*
- 480 2008; **42**: 463–515.
- 2. Dubinsky Z, Stambler N. Photoacclimation processes in phytoplankton: mechanisms,
- consequences, and applications . *Aquat Microb Ecol* 2009; **56**: 163–176.
- 483 3. Wright SW, Jeffrey SW. Pigment Markers for Phytoplankton Production. In: Volkman JK
- (ed). Marine Organic Matter: Biomarkers, Isotopes and DNA. 2006. Springer Berlin
- 485 Heidelberg, Berlin, Heidelberg, pp 71–104.
- 486 4. Armstrong GA. Eubacteria show their true colors: genetics of carotenoid pigment
- biosynthesis from microbes to plants. *J Bacteriol* 1994; **176**: 4795–4802.
- 488 5. Ottesen EA, Young CR, Eppley JM, Ryan JP, Chavez FP, Scholin CA, et al. Pattern and
- synchrony of gene expression among sympatric marine microbial populations. *Proc Natl*
- 490 Acad Sci USA 2013; **110**: E488–E497.
- 491 6. Ottesen EA, Young CR, Gifford SM, Eppley JM, Marin R, Schuster SC, et al. Multispecies
- 492 diel transcriptional oscillations in open ocean heterotrophic bacterial assemblages.
- 493 *Science* 2014; **345**: 207–212.
- 494 7. Aylward FO, Eppley JM, Smith JM, Chavez FP, Scholin CA, DeLong EF. Microbial
- 495 community transcriptional networks are conserved in three domains at ocean basin
- 496 scales. *Proc Natl Acad Sci USA* 2015; **112**: 5443–5448.
- 497 8. Kolody BC, McCrow JP, Allen LZ, Aylward FO, Fontanez KM, Moustafa A, et al. Diel
- 498 transcriptional response of a California Current plankton microbiome to light, low iron, and
- 499 enduring viral infection. *ISME J* 2019; **13**, 2817–2833.
- 500 9. Neveux J, Dupouy C, Blanchot J, Le Bouteiller A, Landry MR, Brown SL. Diel dynamics of

502

503

504

505

506

507

508

509

510

511

512

513

514

515

516

517

518

519

520

521

522

523

chlorophylls in high-nutrient, low-chlorophyll waters of the equatorial Pacific (180°): Interactions of growth, grazing, physiological responses, and mixing. J Geophys Res Ocean 2003; 108: 8140. 10. Le Bouteiller A. Herbland A. Diel variation of chlorophyll a as evidence from a 13-day station in the equatorial Atlantic ocean. *Oceanol Acta* 1982; **5**: 433–441. 11. Litchman E. Resource Competition and the Ecological Success of Phytoplankton. In Falkowski PG , Knoll A *The Evolution of Eukaryotic Phytoplankton*. London and San Diego: Elsevier Academic Press 2007, pp 351–375. 12. Graff JR. Behrenfeld MJ. Photoacclimation Responses in Subarctic Atlantic Phytoplankton Following a Natural Mixing-Restratification Event. Front Mar Sci 2018; 5: 209 Behrenfeld MJ. Boss E. Siegel DA. Shea DM. Carbon-based ocean productivity and 13. phytoplankton physiology from space. Global Biogeochem Cycles 2005; 19: 1–14. 14. Tomkins M, Martin AP, Nurser AJG, Anderson TR. Phytoplankton acclimation to changing light intensity in a turbulent mixed layer: A Lagrangian modelling study. Ecol Modell 2020; **417**: 108917. Wilson ST, Avlward FO, Ribalet F, Barone B, Casev JR, Connell PE, et al. Coordinated 15. regulation of growth, activity and transcription in natural populations of the unicellular nitrogen-fixing cyanobacterium Crocosphaera. Nat Microbiol 2017; 2: 1–9. Emerson S, Quay P, Karl D, Winn C, Tupas L, Landry M. Experimental determination of 16. the organic carbon flux from open-ocean surface waters. Nature 1997; 389: 951-954. 17. Sarmiento JL. Slater R. Barber R. Bopp L. Doney SC. Hirst AC. et al. Response of ocean ecosystems to climate warming. Global Biogeochem Cycles 2004; 18: GB3003.

524 18. Thaben PF, Westermark PO. Detecting Rhythms in Time Series with RAIN. J Biol 525 Rhythms 2014; **29**: 391–400. 526 19. Aylward FO, Boeuf D, Mende DR, Wood-Charlson EM, Vislova A, Eppley JM, et al. Diel 527 cycling and long-term persistence of viruses in the ocean's euphotic zone. Proc Natl Acad 528 Sci USA 2017; 114: 11446-11451. 529 20. Fuhrman JA, Eppley RW, Hagström Å, Azam F. Diel variations in bacterioplankton, 530 phytoplankton, and related parameters in the Southern California Bight. Mar Ecol Prog 531 Ser 1985; 27: 9-20. 532 21. Behrenfeld MJ. Falkowski PG. A consumer's guide to phytoplankton primary productivity models. Limnol Oceanogr 1997; 42: 1479-1491. 533 534 22. Post AF, Dubinsky Z, Wyman K, Falkowski PG. Kinetics of light-intensity adaptation in a marine planktonic diatom. Mar Biol 1984; 83: 231-238. 535 23. Falkowski PG, Kolber Z. Variations in Chlorophyll Fluorescence Yields in Phytoplankton in 536 537 the World Oceans. Funct Plant Biol 1995; 22: 341-355. 538 24. Vaulot D, Marie D. Diel variability of photosynthetic picoplankton in the equatorial Pacific. 539 J Geophys Res Ocean 1999; 104: 3297–3310. 540 25. Nicholson DP, Wilson ST, Doney SC, Karl DM. Quantifying subtropical North Pacific gyre mixed layer primary productivity from Seaglider observations of diel oxygen cycles. 541 542 Geophys Res Lett 2015; 42: 4032-4039. 543 26. Yentsch CS. Distribution of chlorophyll and phaeophytin in the open ocean. Deep Sea Res Oceanogr Abstr 1965; 12: 653–666. 544 Yentsch CS, Reichert CA. The Effects of Prolonged Darkness on Photosynthesis, 27. 545

Respiration, and Chlorophyll in the Marine Flagellate, Dunaliella EUCHLORA. Limnol

546

Oceanogr 1963; 8: 338-342. 547 548 28. Glooschenko WA, Curl Jr. H, Small LF. Diel Periodicity of Chlorophyll a Concentration in 549 Oregon Coastal Waters. J Fish Res Board Canada 1972; 29: 1253–1259. 550 29. Cosper E. Influence of light intensity on diel variations in rates of growth, respiration and 551 organic release of a marine diatom: comparison of diurnally constant and fluctuating light. J Plankton Res 1982; 4: 705-724. 552 553 30. Fouilland E, Courties C, Descolas-Gros C. Size-fractionated phytoplankton carboxylase 554 activities in the Indian sector of the Southern Ocean. J Plankton Res 2000; 22: 1185-555 1201. 556 31. Ragni M, d'Alcalà MR. Circadian variability in the photobiology of Phaeodactylum tricornutum: pigment content. J Plankton Res 2007; 29: 141-156. 557 558 32. Bidigare RR, Buttler FR, Christensen SJ, Barone B, Karl DM, Wilson ST. Evaluation of the utility of xanthophyll cycle pigment dynamics for assessing upper ocean mixing processes 559 560 at Station ALOHA. J Plankton Res 2014; 36: 1423-1433. 561 33. Lichtenthaler HKBT-M in E. Chlorophylls and carotenoids: Pigments of photosynthetic 562 biomembranes. *Plant Cell Membranes*. 1987. Academic Press, pp 350–382. 563 34. Salomon E, Bar-Eyal L, Sharon S, Keren N. Balancing photosynthetic electron flow is critical for cyanobacterial acclimation to nitrogen limitation. Biochim Biophys Acta -564 565 Bioenerg 2013; 1827: 340-347. 566 35. Ünlü C, Drop B, Croce R, van Amerongen H. State transitions in Chlamydomonas 567 reinhardtii strongly modulate the functional size of photosystem II but not of photosystem I. Proc Natl Acad Sci USA 2014; 111: 3460-3465. 568

MacIntyre HL, Kana TM, Anning T, Geider RJ. Photoacclimation of photosynthesis

569

36.

570 irradiance response curves and photosynthetic pigments in microalgae and 571 cyanobacteria. *J Phycol* 2002; **38**: 17–38. 572 37. Karl DM, Church MJ. Microbial oceanography and the Hawaii Ocean Time-series 573 programme. Nat Rev Microbiol 2014; 12: 699–713. 574 38. Becker KW, Collins JR, Durham BP, Groussman RD, White AE, Fredricks HF, et al. Daily 575 changes in phytoplankton lipidomes reveal mechanisms of energy storage in the open ocean. Nat Commun 2018; 9: 5179. 576 577 39. Foy RH, Smith R V. The role of carbohydrate accumulation in the growth of planktonic 578 Oscillatoria species. Br Phycol J 1980; 15: 139–150. 579 40. Cuhel RL, Ortner PB, Lean DRS. Night synthesis of protein by algae. Limnol Oceanogr 1984; **29**: 731–744. 580 581 41. Lacour T, Sciandra A, Talec A, Mayzaud P, Bernard O. Diel variations of carbohydrates and neutral lipids in nitrogen-sufficient and nitrogen-starved cyclostat cultures of 582 isochrysis sp. 1. J Phycol 2012; 48: 966-975. 583 584 42. Lorenzen CJ. A note on the chlorophyll and phaeophytin content of the chlorophyll 585 maximum. Limnol Oceanogr 1965; 10: 482-483. 43. Jeffrey SW. Profiles of photosynthetic pigments in the ocean using thin-layer 586 chromatography. *Mar Biol* 1974; **26**: 101–110. 587 588 44. Head EJH, Horne EPW. Pigment transformation and vertical flux in an area of 589 convergence in the North Atlantic. Deep Sea Res Part II Top Stud Oceanogr 1993; 40: 590 329-346. 591 45. Sun M-Y, Lee C, Aller RC. Anoxic and oxic degradation of 14C-labeled chloropigments 592 and a 14C-labeled diatom in Long Island Sound sediments. Limnol Oceanogr 1993; 38:

594

595

596

597

598

599

600

601

602

603

604

605

606

607

608

609

610

611

612

613

614

615

1438-1451. 46. Champalbert G, Neveux J, Gaudy R, Le Borgne R. Diel variations of copepod feeding and grazing impact in the high-nutrient, low-chlorophyll zone of the equatorial Pacific Ocean (0°; 3°S, 180°). J Geophys Res Ocean 2003; 108. 47. Holzwarth AR, Müller MG, Reus M, Nowaczyk M, Sander J, Rögner M. Kinetics and mechanism of electron transfer in intact photosystem II and in the isolated reaction center: Pheophytin is the primary electron acceptor. Proc Natl Acad Sci USA 2006; 103: 6895— 6900. 48. van Grondelle R. Dekker JP, Gillbro T, Sundstrom V, Energy transfer and trapping in photosynthesis. Biochim Biophys Acta 1994; 1187: 1-65. 49. Shimoda Y, Ito H, Tanaka A. Arabidopsis STAY-GREEN, Mendel's Green Cotyledon Gene, Encodes Magnesium-Dechelatase. Plant Cell 2016; 28: 2147–2160. 50. Baroli I, Niyoqi KK. Molecular genetics of xanthophyll-dependent photoprotection in green algae and plants. Philos Trans R Soc London Ser B Biol Sci 2000; 355: 1385–1394. Andersen RA, Bidigare RR, Keller* MD, Latasa M. A comparison of HPLC pigment 51. signatures and electron microscopic observations for oligotrophic waters of the North Atlantic and Pacific Oceans. Deep Sea Res Part II Top Stud Oceanogr 1996; 43: 517-537. 52. Obata M, Taguchi S. The xanthophyll-cycling pigment dynamics of Isochrysis galbana (Prymnesiophyceae) during light–dark transition. Plankt Benthos Res 2012; 7: 101–110. Sajilata MG, Singhal RS, Kamat MY. The Carotenoid Pigment Zeaxanthin—A Review. 53. Compr Rev Food Sci Food Saf 2008; 7: 29–49.

616 54. Ramel F, Birtic S, Ginies C, Soubigou-Taconnat L, Triantaphylidès C, Havaux M. Carotenoid oxidation products are stress signals that mediate gene responses to singlet 617 oxygen in plants. Proc Natl Acad Sci USA 2012; 109: 5535-5540. 618 619 55. Goss R. Substrate specificity of the violaxanthin de-epoxidase of the primitive green alga 620 Mantoniella squamata (*Prasinophyceae*). *Planta* 2003; **217**: 801–812. 621 56. Viviani DA, Karl DM, Church MJ. Variability in photosynthetic production of dissolved and 622 particulate organic carbon in the North Pacific Subtropical Gyre. Front Mar Sci. 2015;2: 623 73 624 57. Elling FJ. Becker KW. Könneke M. Schröder JM. Kellermann MY. Thomm M. et al. Respiratory quinones in Archaea: phylogenetic distribution and application as biomarkers 625 in the marine environment. Environ Microbiol 2016; 18: 692–707. 626 Becker KW. Elling FJ. Schröder JM. Lipp JS. Goldhammer T. Zabel M. et al. Isoprenoid 627 58. 628 quinones resolve the stratification of redox processes in a biogeochemical continuum 629 from the photic zone to deep anoxic sediments of the Black Sea. Appl Environ Microbiol 630 2018; **84**: e02736-17. 631 59. Nowicka B, Kruk J. Occurrence, biosynthesis and function of isoprenoid guinones. Biochim Biophys Acta 2010; 1797: 1587-1605. 632 633 60. Kruk J, Trebst A. Plastoquinol as a singlet oxygen scavenger in photosystem II. Biochim 634 Biophys Acta 2008; 1777: 154–162. 635 61. Szymańska R, Kruk J. Plastoquinol is the Main Prenyllipid Synthesized During Acclimation to High Light Conditions in Arabidopsis and is Converted to Plastochromanol 636 637 by Tocopherol Cyclase. *Plant Cell Physiol* 2010; **51**: 537–545. 638 62. Agrawal S, Jaswal K, Shiver AL, Balecha H, Patra T, Chaba R. A genome-wide screen in 639 Escherichia coli reveals that ubiquinone is a key antioxidant for metabolism of long chain

640 fatty acids. J Biol Chem 2017; 292; 20086-20099 641 63. Ksas B, Légeret B, Ferretti U, Chevalier A, Pospíšil P, Alric J, et al. The plastoquinone pool outside the thylakoid membrane serves in plant photoprotection as a reservoir of 642 643 singlet oxygen scavengers. Plant Cell Environ 2018; 41: 2277–2287. 644 64. Long SP, Humphries S, Falkowski PG. Photoinhibition of Photosynthesis in Nature. Annu Rev Plant Physiol Plant Mol Biol 1994; 45: 633-662. 645 646 65. Triantaphylidès C, Havaux M. Singlet oxygen in plants: production, detoxification and signaling. Trends Plant Sci 2009; 14: 219-228. 647 648 66. Pospíšil P. Molecular mechanisms of production and scavenging of reactive oxygen species by photosystem II. Biochim Biophys Acta 2012; 1817: 218–231. 649 650 67. Lichtenthaler HK. Biosynthesis, accumulation and emission of carotenoids, α-tocopherol, 651 plastoquinone, and isoprene in leaves under high photosynthetic irradiance. Photosynth 652 Res 2007; 92: 163-179. Shi T, Ilikchyan I, Rabouille S, Zehr JP. Genome-wide analysis of diel gene expression in 653 68. 654 the unicellular N₂-fixing cyanobacterium *Crocosphaera watsonii* WH 8501. *ISME J* 2010; 655 **4**: 621–632. Muñoz-Marín M del C, Shilova IN, Shi T, Farnelid H, Cabello AM, Zehr JP. The 656 69. Transcriptional Cycle Is Suited to Daytime N₂ Fixation in the Unicellular Cyanobacterium 657 658 *"Candidatus* Atelocyanobacterium thalassa" (UCYN-A). *MBio* 2019; **10**: e02495-18. Ashworth J, Coesel S, Lee A, Armbrust EV, Orellana M V, Baliga NS. Genome-wide diel 659 70. 660 growth state transitions in the diatom Thalassiosira pseudonana. Proc Natl Acad Sci USA 2013; **110**: 7518–7523. 661

Smith SR, Gillard JTF, Kustka AB, McCrow JP, Badger JH, Zheng H, et al. Transcriptional

662

71.

Orchestration of the Global Cellular Response of a Model Pennate Diatom to Diel Light 663 Cycling under Iron Limitation. *PLOS Genet* 2016; **12**: e1006490. 664 Harke MJ, Frischkorn KR, Haley ST, Aylward FO, Zehr JP, Dyhrman ST. Periodic and 665 72. 666 coordinated gene expression between a diazotroph and its diatom host. ISME J 2019; 13: 118–131. 667 668 73. Nymark M, Valle KC, Brembu T, Hancke K, Winge P, Andresen K, et al. An Integrated Analysis of Molecular Acclimation to High Light in the Marine Diatom Phaeodactylum 669 670 tricornutum. PLoS One 2009; 4: e7743. 671 74. Kana TM. Geider RJ. Critchlev C. Regulation of photosynthetic pigments in micro-algae 672 by multiple environmental factors: a dynamic balance hypothesis. New Phytol 1997; 137: 629-638. 673 Escoubas J-M, Lomas M, LaRoche J, Falkowski PG. Light Intensity Regulation of cab 674 75. 675 Gene Transcription is Signaled by the Redox State of the Plastoquinone Pool. Proc Natl 676 Acad Sci U S A 1995; 92: 10237–10241. 677 76. White AE, Barone B, Letelier RM, Karl DM. Productivity diagnosed from the diel cycle of particulate carbon in the North Pacific Subtropical Gyre. Geophys Res Lett 2017; 44: 678 3752-3760. 679 680 77. Saito MA, Bertrand EM, Dutkiewicz S, Bulygin V V, Moran DM, Monteiro FM, et al. Iron 681 conservation by reduction of metalloenzyme inventories in the marine diazotroph Crocosphaera watsonii. Proc Natl Acad Sci 2011; 108: 2184–2189. 682 683 78. Marchetti A, Parker MS, Moccia LP, Lin EO, Arrieta AL, Ribalet F, et al. Ferritin is used for 684 iron storage in bloom-forming marine pennate diatoms. Nature 2008; 457: 467. 685 79. Popendorf KJ, Fredricks HF, Van Mooy BAS. Molecular ion-independent quantification of polar glycerolipid classes in marine plankton using triple quadrupole MS. Lipids 2013; 48: 686

185-195. 687 688 80. Collins JR, Edwards BR, Fredricks HF, Van Mooy BAS, LOBSTAHS: An Adduct-Based Lipidomics Strategy for Discovery and Identification of Oxidative Stress Biomarkers. Anal 689 690 Chem 2016; 88: 7154-7162. Hummel J, Sequ S, Li Y, Irgang S, Jueppner J, Giavalisco P. Ultra performance liquid 691 81. 692 chromatography and high resolution mass spectrometry for the analysis of plant lipids. Front Plant Sci 2011; 2: 54. 693 694 82. Smith CA, Want EJ, O'Maille G, Abagyan R, Siuzdak G. XCMS: Processing Mass 695 Spectrometry Data for Metabolite Profiling Using Nonlinear Peak Alignment, Matching. 696 and Identification. Anal Chem 2006; 78: 779–787. 697 83. Kuhl C, Tautenhahn R, Böttcher C, Larson TR, Neumann S. CAMERA: An integrated strategy for compound spectra extraction and annotation of LC/MS data sets. Anal Chem 698 699 2012; **84**: 283–289. 700 84. Bolger AM, Lohse M, Usadel B. Trimmomatic: a flexible trimmer for Illumina sequence data. Bioinformatics 2014; 30: 2114-2120. 701 702 85. Alexander H, Rouco M, Haley ST, Wilson ST, Karl DM, Dyhrman ST. Functional group-703 specific traits drive phytoplankton dynamics in the oligotrophic ocean. Proc Natl Acad Sci 704 USA 2015; 112: E5972-E5979. 705 86. Keeling PJ, Burki F, Wilcox HM, Allam B, Allen EE, Amaral-Zettler LA, et al. The Marine 706 Microbial Eukaryote Transcriptome Sequencing Project (MMETSP): Illuminating the 707 functional diversity of eukaryotic life in the oceans through transcriptome sequencing. 708 PLoS Biol 2014; 12: e1001889. 709 87. Meinicke P. UProC: tools for ultra-fast protein domain classification. *Bioinformatics* 2014;

710

31: 1382–1388.

- 711 88. Li H, Durbin R. Fast and accurate long-read alignment with Burrows–Wheeler transform.
- 712 Bioinformatics 2010; **26**: 589–595.
- 713 89. Anders S, Pyl PT, Huber W. HTSeq—a Python framework to work with high-throughput
- 714 sequencing data. *Bioinformatics* 2014; **31**: 166–169.
- 715 90. Love MI, Huber W, Anders S. Moderated estimation of fold change and dispersion for
- 716 RNA-seq data with DESeq2. Genome Biol 2014; **15**: 550.
- 717 91. Gifford SM, Becker JW, Sosa OA, Repeta DJ, DeLong EF. Quantitative Transcriptomics
- 718 Reveals the Growth- and Nutrient-Dependent Response of a Streamlined Marine
- 719 Methylotroph to Methanol and Naturally Occurring Dissolved Organic Matter. *MBio* 2016;
- **7**: e01279-16.
- 721 92. Mende DR, Bryant JA, Aylward FO, Eppley JM, Nielsen T, Karl DM, et al. Environmental
- drivers of a microbial genomic transition zone in the ocean's interior. *Nat Microbiol* 2017;
- **2**: 1367–1373.

- 724 93. Kiełbasa SM, Wan R, Sato K, Horton P, Frith MC. Adaptive seeds tame genomic
- sequence comparison. *Genome Res* 2011; **21**: 487–493.
- 726 94. Benjamini Y, Hochberg Y. Controlling the False Discovery Rate: A Practical and Powerful
- 727 Approach to Multiple Testing. J R Stat Soc Ser B 1995; **57**: 289–300.
- 728 95. Coenen AR, Hu SK, Luo E, Muratore D, Weitz JS. A Primer for Microbiome Time-Series
- 729 Analysis. Front Genet 2020; **11**: 310.